Angioimmunoblastic T-Cell Lymphoma and Chronic Lymphocytic Leukemia/Small Lymphocytic Lymphoma

A Novel Form of Composite Lymphoma Potentially Mimicking Richter Syndrome

Mounir Trimech, MD, PhD, Audrey Letourneau, PhD,* Edoardo Missiaglia, PhD,* Bernard De Prijck, MD,† Monika Nagy-Hulliger, MD,‡ Joan Somja, MD, PhD,§ Manuela Vivario, MD,§ Philippe Gaulard, MD,‖¶# Frédéric Lambert, MD, PhD,** Bettina Bisig, MD, PhD,* and Laurence de Leval, MD, PhD**

Abstract: Chronic lymphocytic leukemia/small lymphocytic lymphoma (CLL/SLL) is an indolent small B-cell neoplasm that may transform into a clinically aggressive disease, namely Richter syndrome, usually as diffuse large B-cell lymphoma. Besides, CLL/SLL encompasses an increased risk of developing other secondary cancers, including a variety of T-cell lymphomas, often of the anaplastic large-cell type or with a cytotoxic phenotype. Here, we report a small series of patients with composite lymphomas consisting of CLL/SLL and angioimmunoblastic T-cell lymphoma (AITL), a hitherto unrecognized association. The 3 patients (1 male/2 females, 68 to 83 y) presented with high-grade-type symptoms. One patient was clinically suspicious for Richter syndrome, in the others CLL/SLL and AITL were concomitant de novo diagnoses. CLL/SLL and AITL were admixed in the same lymph nodes (3/3 cases) and in the bone marrow (1/2 cases). In all cases, the AITL comprised prominent clear cells with a strong T follicular helper immunophenotype and similar mutations consisting of *TET2* or *DNMT3A* alterations, *IDH2* R172K/M, and *RHOA* G17V. The 3 patients received chemotherapy. One died of early AITL relapse. The other 2 remained in complete remission of AITL, 1 died with recurrent CLL, and 1 of acute myeloid leukemia. These observations expand the spectrum of T-cell lymphoma entities that occur in association with CLL/SLL, adding AITL to the rare variants of aggressive neoplasms manifesting as Richter syndrome. Given that disturbances of T-cell homeostasis in CLL/SLL affect not only cytotoxic but also helper T-cell subsets, these may contribute to the emergence of neoplasms of T follicular helper derivation.

Key Words: composite lymphoma, chronic lymphocytic leukemia/small lymphocytic lymphoma (CLL/SLL), angioimmunoblastic T-cell lymphoma (AITL), Richter syndrome, T follicular helper (TFH) cell, next-generation sequencing

(*Am J Surg Pathol* 2021;45:773–786)

Chronic lymphocytic leukemia/small lymphocytic lymphoma (CLL/SLL), the most common type of leukemia in adults, is composed of small mature $CD5^+$ and $CD23^+$ B cells, with a small proportion of prolymphocytes distributed within proliferation centers in tissue sections. The disease usually runs an indolent clinical course[1]; however, in a subset of patients CLL/SLL may transform into an aggressive disease, either prolymphocytoid transformation (> 55% prolymphocytes in the peripheral blood) or Richter syndrome, a clinically sudden deterioration which occurs in 5% to 10% of the cases.[2–4] In most instances, Richter syndrome corresponds histologically to diffuse large B-cell lymphoma, but a "Hodgkin variant" of Richter syndrome is also recognized, which accounts for a minority of the cases.[5–7]

Although Richter syndrome most often represents clonal evolution of CLL/SLL, which is often associated with *TP53* alterations, less commonly it is the manifestation of a clonally unrelated malignancy, associated with a significantly longer survival than the clonally related cases who tend to do very poorly.[8,9]

Besides, multiple epidemiological studies have shown that CLL/SLL patients are at an increased risk of developing secondary cancers, including other hematological malignancies, cutaneous neoplasms, and solid cancers such as malignant

From the *Department of Laboratory Medicine and Pathology, Institute of Pathology, Lausanne University Hospital and Lausanne University, Lausanne; ‡Service of Hematology, Hospital of Morges, Morges, Switzerland; †Department of Medicine, Division of Hematology; §Department of Pathology, University Hospital of Liège; **Molecular Hemato-Oncology Unit, Center for Human Genetic, UniLab Liège, University Hospital of Liège, Liège, Belgium; ‖Department of Pathology, Henri Mondor Hospital, AP-HP; ¶INSERM U955, Mondor Institute for Biomedical Research (IMRB); and #Paris Est Creteil University, Créteil, France.

B.B. and L.d.L. contributed equally.

Conflicts of Interest and Source of Funding: Supported by a grant of the National Swiss Foundation. The authors have disclosed that they have no significant relationships with, or financial interest in, any commercial companies pertaining to this article.

Correspondence: Laurence de Leval, MD, PhD, Institut de Pathologie, Centre Hospitalier Universitaire Vaudois, 25 rue du Bugnon, Lausanne CH-1011, Switzerland (e-mail: laurence.deleval@chuv.ch).

Supplemental Digital Content is available for this article. Direct URL citations appear in the printed text and are provided in the HTML and PDF versions of this article on the journal's website, www.ajsp.com.

melanoma and carcinomas.[10] Various etiologic factors have been incriminated to account for an increased risk of additional malignancies in CLL/SLL patients, including deregulation of the immune system, shared environmental and genetic factors, and possibly a detection bias caused by attentive patients' surveillance.[11]

The occurrence of cutaneous or systemic T-cell neoplasms in CLL/SLL patients has been documented in several case reports and case series (Table 1).[12–39] Mechanistically, lymphomagenesis has been linked to the accumulation of oligoclonal or monoclonal T-cell populations with abnormal phenotypes or disrupted functional properties commonly observed in CLL/SLL patients.[40,41] Among the 38 systemic T-cell lymphomas reported in CLL/SLL patients so far (Table 1), the majority were diagnosed as peripheral T-cell lymphoma, not otherwise specified (PTCL, NOS),[15,16,18,19,21,23,25,26] anaplastic lymphoma kinase (ALK)-positive anaplastic large-cell lymphoma (ALCL), or ALK-negative ALCL.[14,17–20,24]

Yet, while angioimmunoblastic T-cell lymphoma (AITL) represents one of the most prevalent groups of PTCLs worldwide,[42] to date it has not been reported in association with CLL/SLL. Here, we describe the clinicopathologic characteristics and molecular investigations of 3 patients with composite CLL/SLL and AITL. One patient had long-standing CLL and was clinically suspicious for Richter syndrome, and the other 2, who presented with symptomatic disease, were concomitantly diagnosed with AITL and SLL or CLL, respectively. These observations expand the spectrum of aggressive T-cell lymphomas occurring in association with CLL/SLL and potentially mimicking Richter syndrome.

MATERIALS AND METHODS

Lymphoma Samples and Clinical Data

The 3 cases were identified during diagnostic hematopathology practice at the Institute of Pathology of Lausanne University Hospital. Two cases were outside referrals. All relevant diagnostic materials were reviewed. All samples had been routinely processed by fixation in 10% buffered formalin and paraffin embedding. Consecutive 3-μm-thick sections were used for classic histologic stains, immunohistochemistry, and molecular analyses. The cases were diagnosed following the criteria of the revised 2017 World Health Organization (WHO) classification of lymphoid neoplasms.[1] The clinical history and imaging studies were collected from the patients' files and the treating physicians.

Immunohistochemistry and In Situ Hybridization

Immunohistochemical studies were carried out on formalin-fixed paraffin-embedded (FFPE) tissue using standard protocols routinely applied for diagnostic workup with automated immunostainers (BenchMark XT and Ultra; Ventana Medical Systems, Tucson, AZ). Antibodies against the following antigens were used: CD3 (clone 2GV6; Ventana Medical Systems), CD20 (clone L26; Novocastra, Newcastle, UK), CD79a (clone JCB117, DakoCytomation; Agilent Technologies, Santa Clara, CA), CD2 (clone AB75; Novocastra), CD4 (clone SP35; Ventana Medical Systems), CD5 (clone SP19, Spring Bioscience; Ventana Medical Systems), CD7 (clone CBC37; DakoCytomation), CD8 (clone C8/144B; DakoCytomation), CD10 (clone 56C6; Novocastra), CD19 (clone BT51E; Novocastra), CD21 (clone 1F8; DakoCytomation), CD23 (clone 1B12; Cell Marque, Rocklin, CA), CD30 (clone Ber-H2; DakoCytomation), CD43 (clone DF-T1; DakoCytomation), CD56 (clone CD564; Novocastra), CD138 (clone BA38; Bio-Rad, Hercules, CA), BCL2 (Clone E17; Cell Marque), BCL6 (GI191E/A8; Cell Marque), TIA-1 (clone 2G9A10F5; Beckman Coulter, Brea, CA), granzyme B (clone GrB-7; Monosan, Uden, The Netherlands), CXCL13 (Polyclonal Goat IgG; R&D Systems, Minneapolis, MN), PD1 (polyclonal goat IgG; R&D Systems), ICOS (rabbit polyclonal; Spring Bioscience), TCRb-F1 (clone 8A3; Thermo Fisher Scientific, Waltham, MA), Ki-67 (clone MIB-1; DakoCytomation), kappa, lambda, immunoglobulin (Ig) A, IgG, IgM, IgD (polyclonal rabbit; DakoCytomation). Immunostaining with anti-IDH2 R172K antibody (NewEast Bioscience, King of Prussia, PA) was performed manually.[43]

Chromogenic in situ hybridization for the detection of Epstein-Barr virus (EBV) was performed with Epstein-Barr virus–encoded RNA (EBER) probes (INFORM, EBER Probe; Ventana Medical Systems) and fast red counterstaining, according to the manufacturer's recommendations, with an automated slide stainer (BenchMark XT; Ventana Medical Systems).

Molecular Studies

DNA was extracted from FFPE tissue sections using Maxwell 16 FFPE Plus LEV DNA Purification kit (Promega, Madison, WI) following the manufacturer's instructions, and was quantified by NanoDro 2000 spectrophotometer or Qubit fluorometer (Thermo Fisher Scientific). For each sample analyzed by next-generation sequencing (NGS), B-cell and/or T-cell neoplastic cell contents were estimated, based on morphology and immunostainings. For some specimens, enrichment for areas of interest by manual scraping of toluidine blue-stained sections was performed before DNA extraction for sequencing analyses. DNA quality was assessed by a control ladder polymerase chain reaction (PCR) (100-200-300-400 bp) or by capillary electrophoresis on a Fragment Analyzer System (Agilent Technologies). For patient no. 2, some analyses were also performed on DNA obtained from the fresh-frozen lymph node (LN) sample.

Immunoglobulin and T-Cell Receptor Gene Rearrangements

Lymphoid clonality was studied by multiplex PCRs targeting the immunoglobulin (IG) genes (IGH, IGK, and IGL) and the T-cell receptor (TR) genes (TRB and TRG). We used BIOMED-2 primers (TRB-tubes A/B/C, TRG-tubes A/B, IGH-tubes A/B/C, IGK-tubes A/B, IGL-tube A) with standard PCR conditions[44] with slight modification (40 amplification cycles), plus another set of in-house primers for TRG gene.[45]

TABLE 1. PTCL in CLL/SLL Patients: Summary of Reported Cases

References (No. Cases)	Age/ Sex	CLL vs. SLL	PTCL Type	Time Interval Between CLL and PTCL (Treatment)	Organ Involved by PTCL	Composite Lymphoma	Concurrent CLL/SLL (Location)	Follow-up
This study (3)	68/M	CLL	AITL	6 y (fluda-cyclophosphamide; FCR)	LN	Yes	Yes (LN, BM)	D, 33 mo
	79/F	SLL	AITL	Simultaneous	LN	Yes	Yes (LN)	D, 12 mo
	83/F	CLL	AITL	Simultaneous	LN, BM	Yes	Yes (LN, BM)	D, 24 mo
Abi-Rafeh et al[12] (1)	71/M	CLL	ENKTCL (EBV^+)	Simultaneous: CLL and NK/T-cell lymphoma	Nasal fossa	No	Yes (BM)	A, 96 mo
Roncati[13] (1)	54/M	CLL	PTCL (described as TFH in the paper but only $BCL6^+$, $CD10^-$)	4 y (R-bendamustin)	LN	Yes	Yes	D, few mo
Van Der Nest et al[14] (1)	77/F	CLL	ALCL ALK^+	4 y (no)	LN	Yes	Yes	A, 5 mo
Aoyama et al[15] (1)	77/F	CLL	PTCL-NOS ($CD4^+$)	5 y (fluda)	Blood	Yes	Yes	D, 4 mo
Gorodetskiy et al[16] (1)	40/M	CLL	PTCL-NOS (cytotoxic)	2 y (no)	Salivary gland	Yes	Yes	A, 7 mo
Colling et al[17] (1)	53/M	CLL	ALCL ALK^-	10 y (no)	Testis, buccal mucosae	No	Yes (BM)	D, <1 mo
Mant et al[18] (6)	60/F	CLL	ALCL ALK^-	5 y (FCR)	LN, BM, blood	No	NA	D, 2 mo
	44/M	CLL	ALCL ALK^-	2 y (fluda; CHOP)	LN	No	NA	D, 1 mo
	86/M	CLL	ALCL ALK^-	1 y (no)	Nasal fossa	Yes	Yes (blood)	A, 3 mo
	64/M	CLL	ALCL ALK^+	8 y (FCR)	LN, ascitic fluid, cephalospinal fluid	No	NA	A, 16 mo
	63/F	CLL	ALCL ALK^+	8 y (chlorambucil-prednisone)	LN	No	NA	A, 10 mo
	60/M	CLL	PTCL-NOS (cytotoxic)	Simultaneous	Liver, blood	Yes	Yes	A, 15 mo
Boyer et al[19] (3)	56/F	CLL	ALCL ALK^+	Simultaneous	LN	Yes	Yes	A, 15 mo
	67/F	CLL	ALCL ALK^+	0.8 y (R-CHOP)	LN	No	NA	D, 7 mo
	70/M	CLL	PTCL-NOS (cytotoxic)	11 y (fluda; R-benda)	Spleen	No	Yes (BM)	D, 1 mo
Persad and Pang[20] (1)	47/M	SLL	ALCL ALK^-	Simultaneous	LN	Yes	Yes	A, NA
Alomari et al[21] (1)	68/F	CLL	PTCL-NOS (cytotoxic)	4 y (R-cytoxan-prednisone-vincristine, followed by R-fluda)	LN, BM	Yes	Yes	D, 1 mo
Suefuji et al[22] (1)	80/M	CLL	PTCL	NA (NA)	LN	Yes	Yes	NA
Buddula et al[23] (1)	66/M	CLL	PTCL-NOS (cytotoxic)	6 y (R-fluda-cyclophosphamide)	Maxilla, LN	No	Yes	A, 6 mo
Liu et al[24] (1)	59/M	CLL	ALCL ALK^+	8 y (multiple therapies: chlorambucil-prednisone; fluda; R-fluda; R-pentostatin-cyclophosphamide; R)	LN, BM	Yes	Yes	D, 2 mo
Campidelli et al[25] (2)	80/F	SLL	PTCL-NOS (cytotoxic)	Simultaneous	LN	Yes	Yes	D, 11 mo
	61/M	SLL	PTCL-NOS (cytotoxic)	Simultaneous	BM	Yes	Yes	D, 4 mo
Martinez et al[26] (7)	70/M	CLL	PTCL	13 y (NA)	LN, BM	No	Yes (blood, BM)	NA
	73/M	CLL	PTCL (cytotoxic)	NA (NA)	LN, BM	Yes	Yes (blood, BM)	NA
	59/M	CLL	PTCL (cytotoxic)	< 1 y (fluda)	LN, BM	No	Yes (blood, BM)	NA
	78/M	CLL	MF+NK-cell leukemia	0.8 y (2-chlorodeoxyadenosine)	Skin LN, pleura BM	No	Yes	D, <1mo
	73/M	CLL	PTCL (cytotoxic)	5 y (IL-4)	LN, BM	No	Yes (blood, BM)	A, 7 mo
	57/M	CLL	PTCL (cytotoxic)	14 y (NA)	BM	No	Yes (blood, BM)	NA
	58/M	CLL	PTCL (cytotoxic)	NA (NA)	LN, BM	Yes	Yes (blood, BM)	NA
Martin-Subero et al[27] (1)	69/M	CLL	PTCL (pleomorphic)	6 y (no)	BM, LN, skin, pleura	No	Yes (BM)	D, <1 mo

TABLE 1. (*continued*)

References (No. Cases)	Age/ Sex	CLL vs. SLL	PTCL Type	Time Interval Between CLL and PTCL (Treatment)	Organ Involved by PTCL	Composite Lymphoma	Concurrent CLL/SLL (Location)	Follow-up
Novogrudsky et al[28] (1)	63/M	CLL	PTCL (large cell, $CD4^+$)	10 y (leukeran-prednisone; cytoxan-oncovin-prednisone-fluda)	LN, pancreas, liver, spleen, gallbladder	Yes	Yes	D, <1 mo
Lesesve et al[29] (1)	84/M	CLL	T-large granular lymphocyte leukemia	Simultaneous	Blood, BM	Yes	Yes	D, 8 mo
Nai et al[30] (1)	61/F	CLL	ALCL (ALK status unknown)	3 y (fluda)	Spleen	No	Yes (BM)	NA
Abruzzo et al[31] (1)	74/F	CLL	PTCL (large cell immunoblastic)	6 y (NA)	LN, spleen	No	Yes	D, 74 mo
Lee et al[32] (1)	70/F	CLL	PTCL (large cell immunoblastic)	2 y (NA)	BM	Yes	Yes	D, <1 mo
Liu et al[33] (1)	86/M	SLL	CTCL (small plemorphic T cell/ Sézary)	Simultaneous	LN	Yes	Yes	NA
Strickler et al[34] (2)	65/M	CLL	PTCL (diffuse large T cell)	5 y (NA)	LN, liver, spleen, BM	Yes	Yes	D, <1 mo
	73/M	SLL	PTCL (small pleomorphic T cell)	Simultaneous	LN, BM	Yes	Yes	D, 4 mo

A indicates alive; benda, bendamustine; CHOP, cyclophosphamide-doxorubicine-vincristine-prednisone; D, died; ENKTCL, extranodal natural killer/T-cell lymphoma; F, female; FCR, fludarabine-cyclophosphamide-rituximab; fluda, fludarabine; M, male; MF, mycosis fungoides; NA, not available; NK, natural killer; R, rituximab.

Each reaction was performed in duplicate starting from 75 ng (Nanodrop) or 24 ng (Qubit) of DNA per reaction. Amplification products were analyzed by heteroduplex capillary electrophoresis (QIAxcel, Qiagen, Hilden, Germany) or by capillary electrophoresis on an ABI3500 platform (Thermo Fisher Scientific). Data obtained from the latter were analyzed by means of GeneMapper software version 5 (Thermo Fisher Scientific).

Next-generation Sequencing

High-throughput sequencing analysis was performed using 2 customized panels, 1 covering 26 genes relevant to PTCL biology (*ARID1A*, *ATM*, *BCOR*, *CARD11*, *CCR4*, *CD28*, *CTNNB1*, *DDX3X*, *DNMT3A*, *FYN*, *IDH2*, *IRF4*, *JAK1*, *JAK3*, *KMT2D*, *PIK3CD*, *PLCG1*, *PRKCB*, *RHOA*, *SETD2*, *STAT3*, *STAT5B*, *TET2*, *TNFRSF1B*, *TP53*, *VAV1*), and the other exploring 54 genes of interest in mature B-cell lymphomas (*ARID1A*, *ATM*, *B2M*, *BCL10*, *BCL2*, *BCL6*, *BIRC3*, *BRAF*, *BTK*, *CARD11*, *CCND1*, *CCND3*, *CD274* [*PDL1*], *CD58*, *CD79A*, *CD79B*, *CDK4*, *CDKN2A*, *CIITA*, *CREBBP*, *CXCR4*, *EP300*, *EZH2*, *FOXO1*, *GNA13*, *ID3*, *IRF4*, *KLF2*, *KMT2C*, *KMT2D*, *MAP2K1*, *MAP3K14*, *MEF2B*, *MYC*, *MYD88*, *NFKBIE*, *NOTCH1*, *NOTCH2*, *PDCD1LG2* [*PDL2*], *PIK3CD*, *PLCG2*, *PRDM1*, *PTEN*, *PTPRD*, *REL*, *SF3B1*, *SOCS1*, *STAT6*, *TCF3*, *TNFAIP3*, *TNFRSF14*, *TP53*, *TRAF2*, *XPO1*). Briefly, 100 to 200 ng (Qubit) of DNA template was used to prepare DNA libraries with the KAPA HyperPlus library preparation kit (Roche, Pleasanton, CA). Target enrichment of the DNA libraries was performed by hybridization capture with a custom design of xGen Lockdown Probes (Integrated DNA Technologies, Coralville, IA) covering the full coding sequences of the targeted genes. Enriched libraries were sequenced on an MiSeq™ System (Illumina, San Diego, CA). Sequence analysis was based on established algorithms and pipelines according to GATK best practices (The Genome Analysis Toolkit) standards. Briefly, forward and reverse reads were aligned to the human genome (GATK repository, build 37 decoy) using a BWA aligner (v0.7.5a). BAM files were subjected to PCR duplicate removal (Picard v1.119), followed by realignment around indels and base recalibration using GATK tools (v3.7). Single-nucleotide and indel variant calling was performed using both samtools mpileup (v1.2) and VarScan (v2.3.7), and MuTect2 algorithm (GATK v3.7). The union of the variant calls were annotated for presence in dbSNP and COSMIC databases and mutation effect on gene transcript by SnpEff (v.4.3). Further variant filtering was carried out in R, keeping variants that showed an allele frequency $>1\%$, having at least 50 reads supporting the reference sequence and >5 reads supporting the variant. A filter based on a list of known artifacts was also applied. All retained alterations were confirmed by visual inspection with the Integrative Genomics Viewer (IGV) tool.

RESULTS

Clinical Histories

Patient No. 1

A 62-year-old man was diagnosed in 2006 with Rai stage IV CLL, with a normal karyotype and hypermutated IG heavy chain gene. Treatment with 6 cycles of fludarabine/cyclophosphamide resulted in complete response. In 2010, the patient developed slowly progressive LN enlargement and anemia, which resolved after 4 cycles of fludarabine/

cyclophosphamide/rituximab administered in early 2011. In February 2012, he presented with a worsening general condition, B symptoms, enlargement of supradiaphragmatic and infradiaphragmatic LNs, bone pain, pancytopenia, and IgM paraprotein (15 g/L). The positron emission tomography (PET)-computed tomography (CT) scan showed hypermetabolic disseminated lymphadenopathy, splenomegaly (16 cm), and diffuse heterogenous increase in bone marrow (BM) uptake. A Richter syndrome was suspected. A BM trephine biopsy showed multifocal nodular infiltration by the CLL. A cervical LN biopsy was diagnosed as a composite infiltrate by CLL in association with an AITL. The patient then received 2 full doses and 1 attenuated cycle of etoposide, high-dose cytarabine, and cisplatin, leading to a metabolic response with persistence of cervical adenopathy and an IgM paraprotein at 0.5 g/L. In July 2012, the patient underwent splenectomy (involved by the CLL without evidence of AITL), followed by a nonfamilial mini-allograft. Control PET-CT was negative, and BM immunophenotyping contained minimal residual disease (0.9%) with no atypical T cells. In August 2013, generalized lymphadenopathy recurred, while the BM contained 40% clonal B cells. An axillary LN biopsy showed relapse of the CLL. Administration of GEMOX (gemcitabine, oxaliplatin) induced a partial response, and the patient was switched to R-CHOP (rituximab, cyclophosphamide, doxorubicin, vincristine, and prednisone) with perfusion of donor lymphocytes (donor lymphocyte infusion), leading to a complete response in June 2014. In November 2014, the patient passed away in a poorly documented context of respiratory infection.

Patient No. 2

A 79-year-old woman with multiple comorbidities (ischemic heart disease, chronic renal insufficiency, and nutritional deficiency) presented in October 2013 with painful cervical tumefaction and B symptoms. Clinical examination and CT scan found disseminated lymphadenopathy and moderate splenomegaly. White blood cell count was 1.54 g/L (70.7% neutrophils, 10.3% lymphocytes, and 12.2% eosinophils), and other blood tests showed elevated lactate dehydrogenase levels (486 U/L) and C-reactive protein (104 mg/L). A 3.5 cm cervical LN biopsy led to the diagnosis of composite involvement by SLL and AITL. BM biopsy was not performed. The patient received 6 cycles of CHOP between November 2013 and March 2014, with complete remission after 4 cycles. However, she remained in a weakened general condition with anemia. An upper digestive endoscopy, performed in October 2014 because of epigastric pain, found antral and angular ulcers and histology showed involvement by AITL. No additional treatment was administered and the patient expired a few days later.

Patient No. 3

An 83-year-old woman with a history of breast carcinoma treated by surgery and chemotherapy in 1977 was admitted to the hospital in February 2018 for investigation of a rapidly worsening general condition with B symptoms, productive cough, and skin rash. Blood analysis disclosed lymphocytosis at 14.3 g/L and CT scan showed multiple supradiaphragmatic and subdiaphragmatic lymphadenopathies. PET-CT evidenced hypermetabolic LNs with maximal standardized uptake values at 16, splenic hypermetabolism (maximum standardized uptake value = 7), and multiple suspect skin nodules. A 4.2 cm inguinal LN biopsy and the BM biopsy both showed composite involvement by AITL and CLL. Because of the poor performance status, monotherapy by bendamustine (120 mg/m^2) was initiated in March 2018. After 5 cycles of treatment (August 2018), PET-CT indicated complete metabolic remission, and white blood cell counts had normalized. In September 2019, a follow-up PET-CT showed tonsillar hypermetabolism prompting bilateral tonsillectomy. Histologic analysis evidenced benign lymphoid hyperplasia, scattered EBV-positive cells, and *Actinomyces* colonization, but no evidence of AITL or CLL. A BM biopsy, performed in 2019 due to progressive bicytopenia, disclosed an acute myeloid leukemia (AML) with a minimal residual CLL infiltrate. The patient refused further treatment and died in February 2020 of community-acquired pneumonia.

Morphology and Immunohistochemical Features

Patient No. 1

The 2006 LN biopsy (Supplementary Figs. 1a–k, Supplemental Digital Content 1, http://links.lww.com/PAS/B54) showed a diffuse infiltrate of small lymphocytes with proliferation centers, histologically typical for CLL. By immunohistochemistry, the lymphoma cells were CD20$^+$, CD5$^+$, CD43$^+$, CD23$^{-/+}$, IgM$^+$, IgD$^+$, kappa, with a Ki-67 proliferative index <5%. No plasma cell differentiation was seen.

The 2012 cervical LN (Fig. 1) was entirely involved by a diffuse lymphoproliferation comprising small foci of necrosis, focally extending into the perinodal fat while sparing the peripheral cortical sinus. The polymorphous infiltrate was predominantly composed of small-sized to medium-sized lymphoid cells with plasmacytoid differentiation, sometimes with Dutcher bodies, plasma cells, and scattered large blastic cells. In addition, there was a distinct subset of atypical medium-sized cells, with moderately abundant clear cytoplasm, isolated or in small clusters, featuring rather numerous and sometimes atypical mitoses. Prominent arborizing venules were seen. There was no significant eosinophilia. By immunohistochemistry (Figs. 1D–L), the majority of the infiltrate consisted of CD19$^+$, CD20$^{-/+}$, CD79a$^+$, CD5$^+$, CD43$^+$ B cells. The B cells and plasma cells were positive for IgM and IgD with kappa light-chain restriction. CD20 and CD23 also underlined the scattered blastic cells, which coexpressed CD30, IgM, IgD, and kappa. The aggregates of medium-sized clear cells were CD3$^+$, CD2$^+$, CD5$^+$, CD7$^-$, CD4$^+$, CD8$^-$ expressed several T follicular helper (TFH)-cell markers (CD10, CXCL13, ICOS, and PD1), and were topographically related to an irregularly expanded CD21$^+$ follicular dendritic cell (FDC) meshwork. Only a few scattered small lymphocytes were EBER-positive.

The 2012 BM biopsy (not shown) was about 50% cellular, with reduced trilinear hematopoiesis and a multifocal nodular CLL infiltrate (CD20$^+$, CD5$^+$, CD23$^{-/+}$, IgM$^+$, IgD$^+$, kappa), with slight plasma cell differentiation. The spleen removed in July 2012 (Supplementary Figs. 1l–p, Supplemental Digital Content 1, http://links.lww.com/PAS/B54) showed

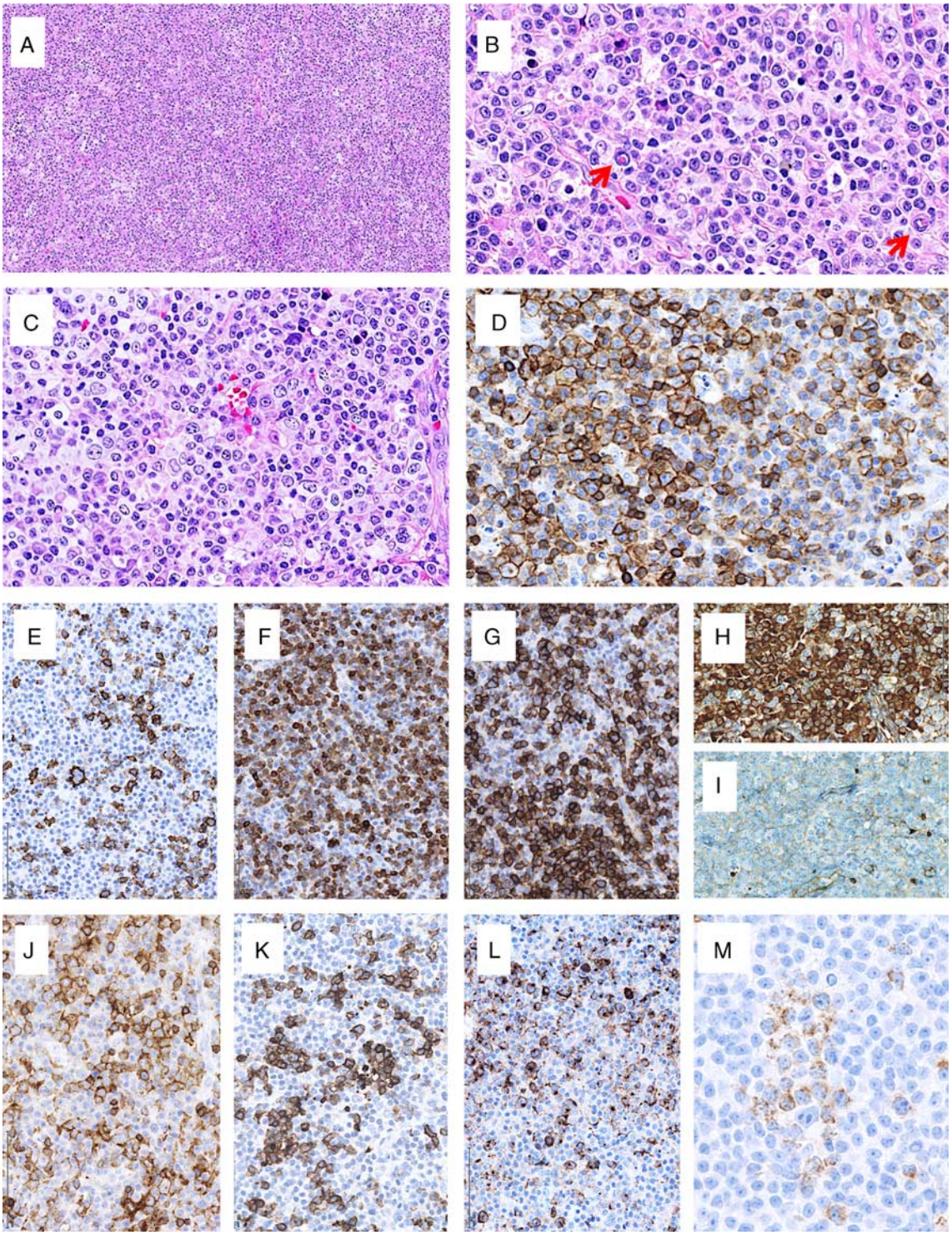

FIGURE 1. Histopathology of the 2012 LN biopsy with composite lymphoma from patient no. 1. A, The LN architecture was effaced by a diffuse lymphoproliferation (hematoxylin and eosin). B, The polymorphic lymphoid infiltrate comprised numerous lymphoplasmacytoid cells and plasma cells, sometimes with Dutcher bodies (arrows), numerous scattered blasts and aggregates of medium to large cells with abundant clear cytoplasm, admixed with arborized vessels (hematoxylin and eosin) (C). D, CD5 stained strongly scattered small T cells and the large atypical clear cells, and stained weakly a diffuse infiltrate of small B cells. E, CD20 stained partially and weakly the small B cells and strongly scattered large cells. F, CD79a stained more extensively a B-cell component. G, CD138 highlighted numerous plasma cells, which were positive for kappa light chain (H), and negative for lambda (I). J, The atypical clear cells were $CD4^{+}$, with coexpression of CD10 (K) and ICOS (L). M, Immunostaining for the IDH2 R172K mutant protein showing a strong cytoplasmic positive signal in atypical cells.

nodular and diffuse infiltrate of white and red pulps by CLL ($CD20^+$, $CD43^+$, $BCL2^+$, IgM^+, IgD^+, kappa, Ki-67 15%), with a monotypic plasma cell component and no evidence of either transformation into a large B-cell lymphoma or atypical T cells. The 2013 LN biopsy (not shown) showed a relapse of CLL ($CD20^+$, $CD5^+$, $CD23^+$, $CD43^+$, IgM^+, IgD^+, kappa) with slight plasma cell differentiation.

Patient No. 2

The LN (Fig. 2) showed capsular fibrosis, irregular fibrous bands, and a vaguely nodular heterogenous lymphoid infiltrate. Most areas consisted of a polymorphic lymphoid population comprising numerous atypical large, medium-sized, and smaller cells, showing numerous mitotic figures, associated with a prominent proliferation of branching high endothelial venules. Those areas also included numerous eosinophils, plasma cells, and histiocytes, and showed multiple small foci of necrosis. In several places, there was an abrupt transition into distinctively more basophilic regions composed of a monotonous and dense population of small lymphocytes focally admixed with prolymphocytes and paraimmunoblasts. By immunohistochemistry (Figs. 2E–J), the compact aggregates of small lymphoid cells were positive for CD20 and CD79a, with coexpression of CD5, CD23, and CD43, and IgM lambda surface Ig restriction. In the polymorphous areas, the majority of the atypical cells were $CD3^+$, $CD4^+$, $CD2^+$, $CD7^-$, $CD8^-$, $TCRb\text{-}F1^+$ T cells with a TFH immunophenotype (positive for CD10, CXCL13, PD1, and ICOS). There were also a few large $CD20^+$ and $CD30^+$ immunoblasts with cytoplasmic expression of IgM and lambda. CD21 highlighted scattered aggregates of FDCs, overall rather limited. Ki-67 proliferation index was 25% to 30% and in situ hybridization for EBER was negative. Cytogenetic analyses showed a 19q13 deletion, suggesting a t (14;19)(q32;q13) translocation involving *BCL3* gene.

The gastric biopsies (Supplementary Fig. 2, Supplemental Digital Content 2, http://links.lww.com/PAS/B55) were infiltrated by atypical pleomorphic medium-sized lymphoid cells and numerous eosinophils. By immunostaining, there were essentially no $CD20^+$ cells. The atypical cells were $CD2^+$, $CD3^+$, and $CD4^+$ T cells coexpressing CD10, ICOS, and CXCL13.

Patient No. 3

The inguinal LN (Fig. 3) was effaced by a diffuse polymorphic lymphoproliferation consisting of atypical, mostly medium-sized lymphoid cells with pale cytoplasm, admixed with scattered large blastic cells. The atypical cells were arranged in large sheets, sometimes surrounding hyperplastic and congested blood vessels, admixed with a few eosinophils and some plasma cells. Besides, there were dense clusters of monotonous small lymphocytes with scant cytoplasm and basophilic nuclei with clumped chromatin. By immunohistochemistry (Figs. 3D–J), the atypical clear cells were $CD2^+$, $CD3^+$, $CD4^+$, $CD5^+$, $CD7^-$ with a TFH phenotype ($BCL6^+$, $CD10^+$, $PD1^+$, $ICOS^+$, $CXCL13^{-/+}$) and partial expression of CD30. CD21 showed large, irregularly expanded FDC meshworks. CD20 stained few large cells and the small cell component. The latter was also $CD5^+$, $CD23^+$, $CD43^+$, $LEF1^+$, IgG^+ kappa. The majority of the plasma cells in the T-cell areas were positive for IgG and kappa. EBER in situ hybridization was positive in a small number of blasts.

The staging BM biopsy (2018) (Figs. 3B, C) was hypercellular (85%) and showed about 60% infiltration by a lymphoid component, mostly consisting of CLL cells ($CD20^+$, $CD23^+$, $CD5^+$, $LEF1^+$) admixed with aggregates of medium to large clear cells. The latter were $CD3^+$, $CD4^+$, $BCL6^+$, $PD1^+$, $ICOS^+$, with partial expression of CD10 and CXCL13. No monotypic plasma cell component was identified.

Bilateral tonsillectomy (not shown) showed reactive follicular hyperplasia, scattered interfollicular $CD30^+$ blasts, mild polytypic plasmocytosis, and colonies of actinomyces. A few EBER-positive cells of variable size were present.

The 2019 BM aspirate and biopsy (not shown) were hypercellular (65%) and mostly infiltrated by medium-sized blasts with a myeloid/monocytoid appearance, representing from 25% to 40% (aspirate) up to 60% (biopsy) of the marrow cellularity. By flow cytometry and immunohistochemistry, the blasts were $CD34^+$, $HLA\text{-}DR^+$, $CD117^+$, $CD38^+$, $CD33^+$, $CD13^{+/-}$, MPO^+, $CD68^{-/+}$, without significant p53 expression. Residual hematopoiesis was reduced, showing dysplastic morphologic features, without reticulin fibrosis. Immunostainings showed a minimal CLL component (10%) ($CD79a^+$, $CD20^-$, $CD5^+$, $CD23^+$, $LEF1^+$), and no evidence of residual AITL infiltration. Conventional cytogenetics showed a 47,XX karyotype, including an additional small marker chromosome of unknown origin (47,XX,+mar), in 8 of 20 analyzed metaphases. A DNA-based hotspot NGS panel (custom AmpliSeq. 52 gene panel, Thermo Fisher Scientific) showed no mutation. In particular, no *TP53* or *NRAS* gene mutation was evidenced. An RNA-based NGS assay (Oncomine Myeloid Research assay, Thermo Fisher Scientific) detected no recurrent fusion gene.

Molecular Findings

PCR-based analyses of the IG and TR gene rearrangements and targeted deep sequencing with the T-cell lymphoma panel were carried out on all relevant available biopsy samples with available good quality DNA. NGS with the B-cell lymphoma panel was performed on the LN with composite lymphoma. Results are summarized in Table 2 and are illustrated in Figure 4.

Overall, the clonality assays supported the histopathologic conclusions. In the 3 cases, the LN interpreted to contain CLL or SLL plus AITL indeed harbored dual IG and TR gene rearrangements. In patient no. 1, the same monoclonal IG gene rearrangements were also detected in the earlier LN biopsy and in the subsequent samples (spleen 2012 and LN 2013) involved by the CLL, whereas the monoclonal TR gene rearrangement was not found in any of these samples. In gastric biopsies of patient no. 2, interpreted as recurrent AITL, only monoclonal TR gene rearrangements were detected, similar to those of the LN biopsy, whereas a polyclonal pattern was observed for IG genes. In patient no. 3, the same monoclonal IG and TR rearrangements were amplified in the LN and the staging BM, and were not found in the tonsils.

NGS analysis by means of the T-cell lymphoma panel disclosed a mutational pattern very characteristic of AITL in the 3 composite samples. The 3 cases had in common

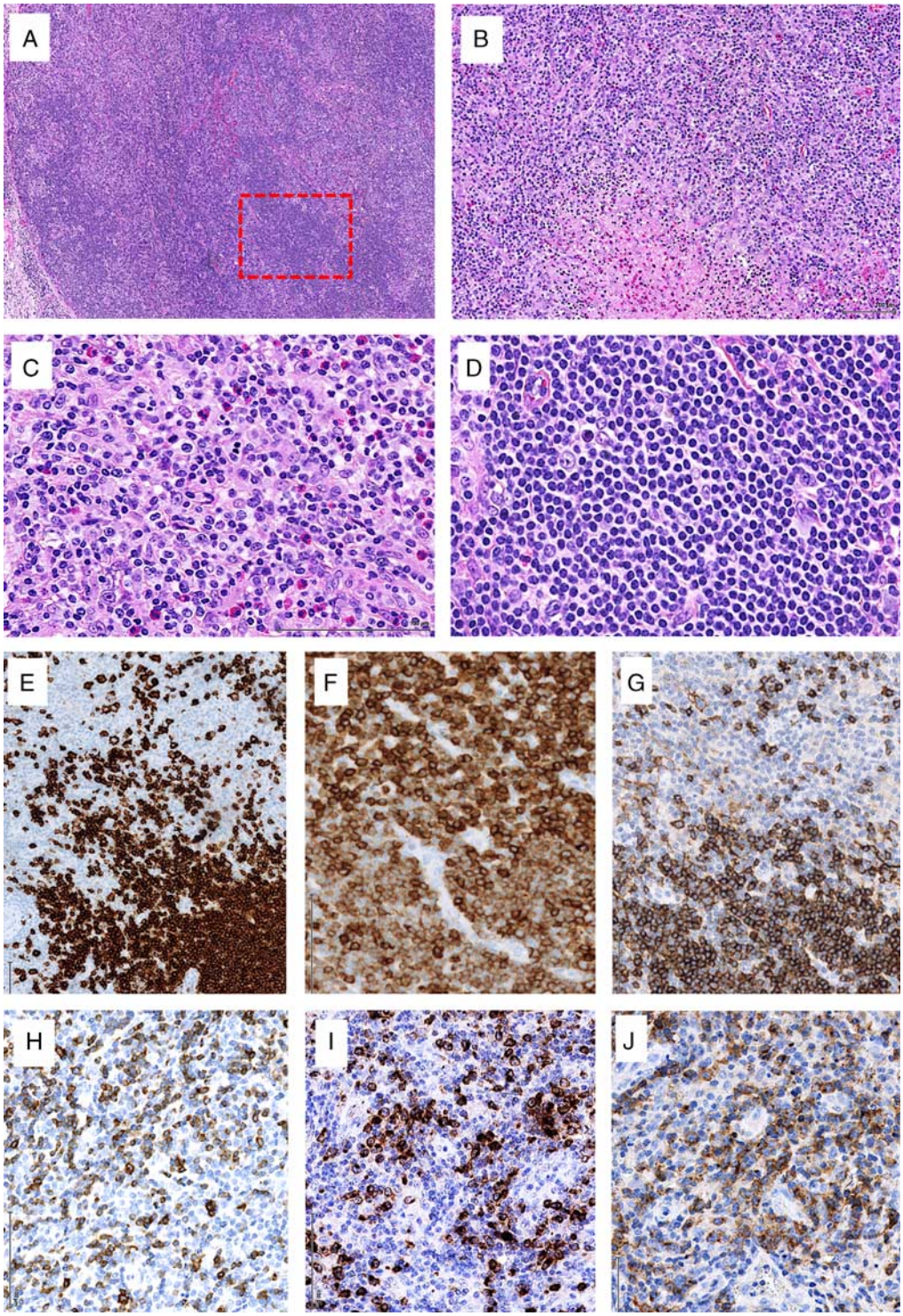

FIGURE 2. Histopathology of the LN with composite lymphoma from patient no. 2. A and B, The LN architecture was effaced by a diffuse lymphoid infiltrate with vaguely nodular appearance, and presence of a few incomplete fibrous bands and small foci of ischemic necrosis (hematoxylin and eosin). C, The lymphoid proliferation is richly vascularized and composed of polymorphic cells rich in large blasts, mixed with smaller, intermediate and small cells with irregular nuclei, associated with eosinophils and some histiocytes (hematoxylin and eosin). D, High magnification of the boxed areas in (A) showed a monotonous population of small mature lymphocytes admixed to some prolymphocytes and paraimmunoblasts (hematoxylin and eosin). Immunostains for CD20 (E), CD5 (F), and CD23 (G) highlighted small lymphoid cells. H, The atypical cells in the polymorphous areas were $CD4^+$, $CXCL13^+$ (I), and $PD1^+$ (J).

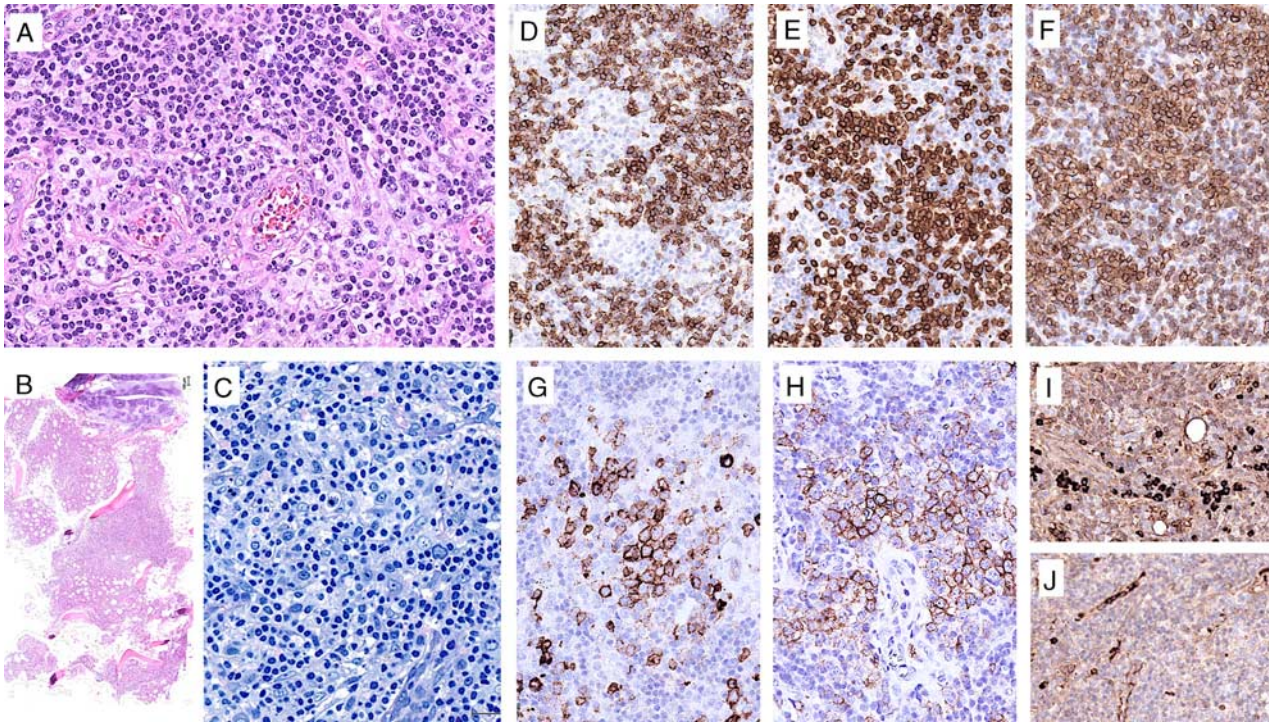

FIGURE 3. Histopathology of the LN and BM with composite lymphoma from patient no. 3. A, The LN comprised aggregates of medium to large clear cells in the vicinity of turgescent blood vessels and a monotonous infiltrate of small lymphoid cells (hematoxylin and eosin). B and C, The BM was hypercellular and contained an infiltrate composed of small lymphoid cells and large pale cells (hematoxylin and eosin and Giemsa). D, CD20 stained the small lymphoid cells, whereas CD3 stained the large clear cells (E). F, Both components were $CD5^+$. Atypical T cells were $CD10^+$ (G) and $PD1^+$ (H). Immunostains for kappa (I) and lambda (J) showed monotypic plasma cells.

the pathogenic *RHOA* p.G17V mutation, a pathogenic *IDH2* mutation at the hotspot position R172 (p.R172K or p.R172M), and 2 or 3 *TET2* nonsense or frameshift mutations, likely pathogenic. Samples from patient nos 2 and 3 also contained a mutation in *DNMT3A* (p.R882H, pathogenic and p.E561*, likely pathogenic, respectively). Variant allele frequencies (VAFs) of these AITL-associated mutations were variable but generally low, in accordance with the neoplastic T-cell content in the samples. They ranged from 2% to 20% in the primary composite samples, with the higher VAFs in genes (*DNMT3A* and *TET2*) that have been reported mutated in clonal hematopoiesis of indeterminate potential (CHIP), suggesting that a CHIP clone may coexist in those cases. As an alternative explanation to the higher VAFs of *DNMT3A* and *TET2* gene mutations, it cannot be excluded that the latter occurred earlier in the development of the T-cell clone, before *RHOA* or *IDH2* mutations.

In patient no. 1, immunostaining with an antibody specific for the R172K IDH2 mutant protein confirmed cytoplasmic granular positivity in atypical clear cells (Fig. 1M). None of the AITL-associated variants were detected either at the initial diagnosis of CLL (LN 2006) or in the consecutive relapses of CLL (spleen 2012, LN 2013). Conversely, a nonsense mutation in *DDX3X* (p.G29*, likely pathogenic) was present in all analyzed samples, including those infiltrated by the CLL only and before the diagnosis of composite lymphoma. This variant, found at a high VAF in all samples (31% to 85%), was likely associated with the CLL. The B-cell lymphoma NGS panel showed 2 additional mutations related to the CLL component, with VAFs consistent with this hypothesis: *SF3B1* p.G740V and *BRAF* p.G469A. In patient no. 2, the same mutational profile was detected in gastric biopsies, involved by AITL, as in the diagnostic LN. Most VAFs in the stomach were very low, but consistent with the neoplastic cell burden in that tissue. The B-cell lymphoma panel did not evidence additional mutations in the LN. In patient no. 3, identical mutational profiles were found in the LN and the concomitant BM. An *EZH2* mutation of uncertain functional significance (p.R347W) was detected by the B-cell lymphoma panel in the LN, at a VAF of 5%, but it is uncertain to which neoplastic component this finding should be attributed to. NGS analysis of the tonsil removed later showed mutations of *TET2* and *DNMT3A* similar to those detected earlier in the LN and BM, at low VAFs (1% to 2%), consistent with CHIP. No mutation was detected by means of the T-cell lymphoma panel in the AML (including the absence of any *TP53* gene mutation).

DISCUSSION

The 3 cases of composite CLL/SLL and AITL described here expand the spectrum of systemic T-cell neoplasms occurring in association with CLL/SLL, summarized in Table 1. As the first 2 cases of nodal PTCL occurring in

TABLE 2. Summary of Clonality and Sequencing Analyses

Case Number	Tissue (Sampling Date)	Diagnosis (Tumor Cell Content)	Clonality Assays*		NGS T-Cell Lymphoma Panel				NGS B-Cell Lymphoma Panel			
			IG	TR	Mean Coverage	Mutations Gene	Variant	VAF	Mean Coverage	Mutations Gene	Variant	VAF
Patient No.1	Lymph node (10/2006)	CLL (85%)	Clonal[1] (IGH IGK)	Polyclonal	351X	*DDX3X*	c.85G>T (p.G29*)	85%			ND	
	Lymph node (02/2012)	CLL (70%) & AITL (10%)	Clonal[1] (IGH IGK)	Clonal (TRG)	1722X	*DDX3X*	c.85G>T (p.G29*)	62%	1123X	*SF3B1*	c.2219G>T (p.G740V)	35%
						TET2	c.2896C>T (p.Q966*)	8%		*BRAF*	c.1406G>C (p.G469A)	22%
						TET2	c.3434del (p.G1145Vfs*7)	5%				
						IDH2	c.515G>A (p.R172K)	4%				
						RHOA	c.50G>T (p.G17V)	3%				
	Spleen (07/2012)	CLL (40%)	Clonal[1] (IGH IGK)	Polyclonal	125X	*DDX3X*	c.85G>T (p.G29*)	31%			ND	
	Lymph node (08/2013)	CLL (85%)	Clonal[1] (IGH IGK)	Polyclonal	2736X	*DDX3X*	c.85G>T (p.G29*)	82%			ND	
Patient No.2	Lymph node (10/2013)	CLL (10%) & AITL (20%)	Clonal (IGH IGK IGL)	Clonal[2] (TRB TRG)	3562X	*DNMT3A*	c.2645G>A (p.R882H)	20%	1487X		WT	
						TET2	c.1061del (p.S354*)	19%				
						TET2	c.2290dup (p.Q764Pfs*5)	9%				
						RHOA	c.50G>T (p.G17V)	9%				
						IDH2	c.515G>T (p.R172M)	7%				
						TET2	c.2279_2283dup (p.H762Ffs*53)	2%				
	Stomach (10/2014)	AITL (10%)	Polyclonal	Clonal[2] (TRB TRG)	778X	*DNMT3A*	c.2645G>A (p.R882H)	23%			ND	
						TET2	c.1061del (p.S354*)	23%				
						TET2	c.2290dup (p.Q764Pfs*5)	2%				
						RHOA	c.50G>T (p.G17V)	2%				
						IDH2	c.515G>T (p.R172M)	1%				
						TET2	c.2279_2283dup (p.H762Ffs*53)	0.5%†				
Patient No.3	Lymph node (02/2018)	CLL (20%) & AITL (20%)	Clonal[3] (IGH IGK)	Clonal[4] (TRG)	1240X	*DNMT3A*	c.1681G>T (p.E561*)	11%	2103X	*EZH2*	c.1039C>T (p.R347W)	5%
						TET2	c.2290dup (p.Q764Pfs*5)	11%				
						IDH2	c.515G>T (p.R172M)	9%				
						RHOA	c.50G>T (p.G17V)	7%				
						TET2	c.1648C>T (p.R550*)	6%				
	Bone marrow (02/2018)	CLL (20%) & AITL (10%)	Clonal[3] (IGH IGK)	Clonal[4] (TRG)	960X	*TET2*	c.2290dup (p.Q764Pfs*5)	11%			ND	
						DNMT3A	c.1681G>T (p.E561*)	5%				
						RHOA	c.50G>T (p.G17V)	2%				
						TET2	c.1648C>T (p.R550*)	1%				
						IDH2	c.515G>T (p.R172M)	1%				
	Tonsils (09/2019)	Benign lymphoid hyperplasia	Polyclonal	Polyclonal	1776X	*DNMT3A*	c.1681G>T (p.E561*)	2%			ND	
						TET2	c.2290dup (p.Q764Pfs*5)	1%				
						TET2	c.1648C>T (p.R550*)	1%				
	Bone marrow (10/2019)	CLL (10%) & AML (60%)	ND	ND	2318X		WT				ND	

*For clonality assays, identical clones are annotated with the same superscript numbers (1 to 4).
†Mutation identified by visual inspection on Integrative Genomics Viewer (IGV).
ND indicates not done; WT, wild-type.

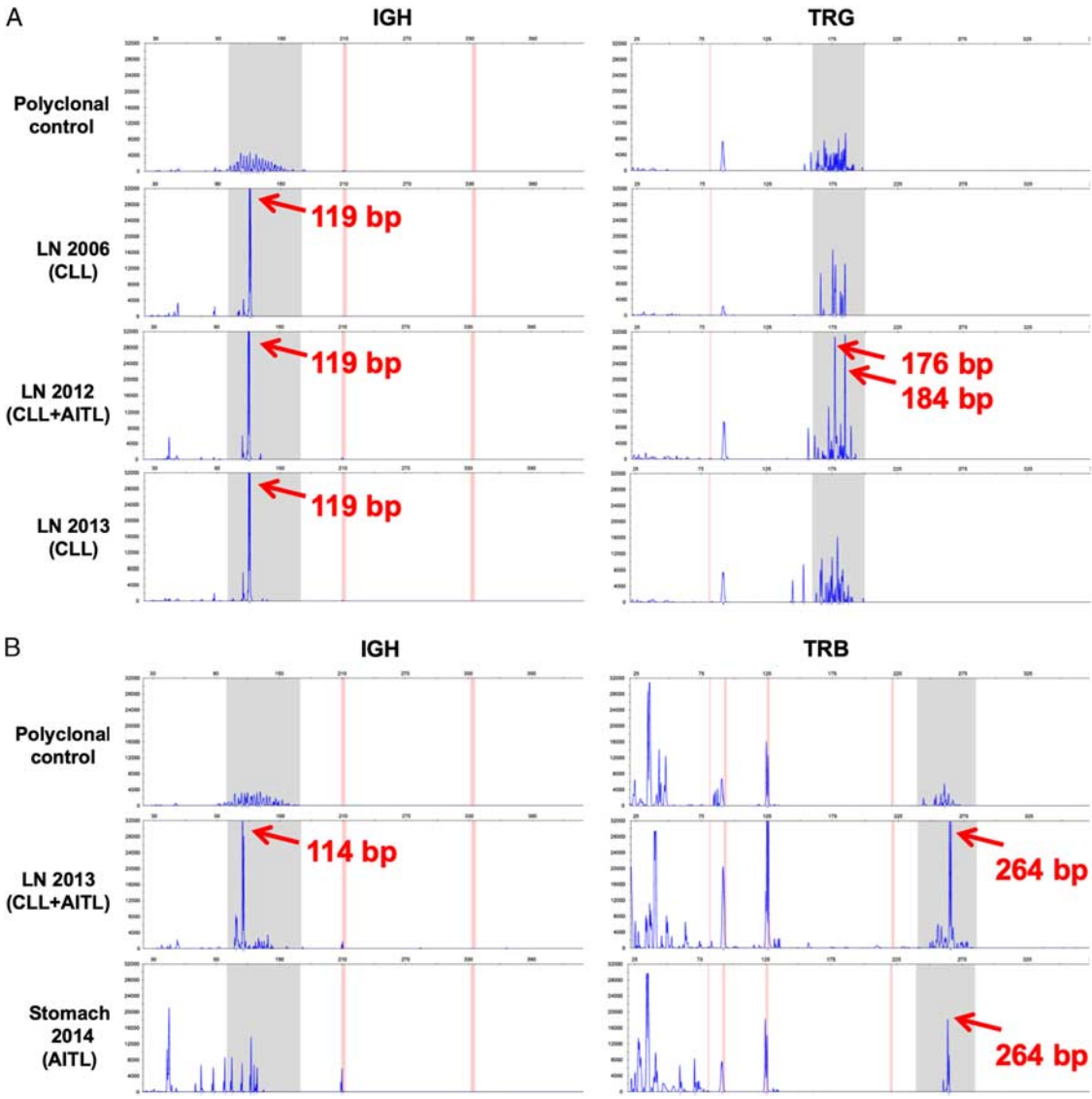

FIGURE 4. Representative GeneScan results of the IG and TR gene rearrangement analyses in a control sample and different successive biopsy samples for patient no. 1 (A) and patient no. 2 (B). Arrows indicate monoclonal peaks. The gray-colored areas correspond to the expected molecular size ranges of amplification products. The vertical pink lines indicate the theoretical localization of potential nonspecific amplifications.

patients with CLL or SLL were reported in 1992 by Strickler et al,[34] 36 additional cases have been published in the literature. The patients with CLL (33 cases) or SLL (5 cases) were 27 men and 11 women, and were diagnosed with PTCL at a median age of 69 years (40 to 86 y). The majority of the patients (22/35) had a history of CLL/SLL known for 2 to 14 years (median: 5 y) and a smaller subset of patients (13/35) were diagnosed simultaneously or within a short-time interval (< 1 y) with CLL/SLL and PTCL. Most cases (21/38) consisted of composite lesions comprising both PTCL and CLL/SLL in the same biopsy,[13–16,18–22,24–26,28,29,32–34] whereas in the other cases (17/38) the PTCL tissue did not contain the CLL/SLL component.[12,17–19,23,26,27,30,31] The majority of cases (22/38) were qualified as PTCL or PTCL, NOS, often with a cytotoxic phenotype (in 12 cases), 12/38 cases were ALCLs (6 ALK-positive, 5 ALK-negative, and 1 ALK status unknown), and there were 1 case each of aggressive EBV-negative natural killer–cell leukemia, EBV-positve nasal natural killer/T-cell lymphoma, T-large granular lymphocyte leukemia, and nodal lymphoma with a TFH cell phenotype. Regarding the latter case,[13] however, the information provided in the case report does not fully support the proposed diagnosis as only 1 TFH marker (BCL6) is reported positive in a lymphoma otherwise lacking morphologic features that might suggest a TFH derivation.[46]

The features of the T-cell neoplasms diagnosed in association with CLL/SLL in our 3 patients were morphologically typical of AITL, a diagnosis that was

further supported by the demonstration of a strong TFH immunophenotype and a constellation of mutations characteristic of that disease and remarkably similar in the 3 cases, including *TET2* or *DNMT3* alterations, *IDH2* p. R172K/M and *RHOA* p.G17V mutations.[47–50] Interestingly, these 3 cases also exemplified typical large clear-cell cytology, a feature that was recently reported as characteristic of *IDH2*-mutated AITL.[51]

A striking feature of the composite lymphoma in patient no. 1 was the massive plasmacytoid and plasma cell differentiation of the CLL component in association with the AITL. In fact, typical CLL was not seen in that biopsy and knowledge of the preceding history was clue to a correct interpretation. Curiously, plasmacytoid differentiation was not observed at the time of the diagnosis of CLL and persisted to a lesser extent in the subsequent splenectomy involved by CLL only, suggesting that it could have been induced by the AITL component. A similar phenomenon was observed in composite lesions of the other 2 patients. The large B cells in patient no. 2 and the plasma cells in association with the AITL areas in patient no. 3 showed cytoplasmic expression of the same Ig light and heavy chains as the CLL/SLL. In fact, normal TFH cells physiologically provide help for B-cell differentiation and plasma cell differentiation.[52] This property, mediated by various cytokines such as interleukin (IL)-6, IL-10, and IL-21, is to some extent retained in TFH neoplasms, and AITL is well known to encompass various degrees of EBV-positive or EBV-negative B cell or plasma cell expansions, which are usually polyclonal or sometimes monoclonal.[1,53,54] Typically, this B-cell population consists of a minority of large EBV-positive B cells, which may occasionally progress to an EBV-positive diffuse large B-cell lymphoma.[53] Interestingly, EBV-negative B-cell lymphoproliferations associated with AITLs and other PTCLs have been found to encompass a spectrum of clonal or monotypic lesions ranging from plasma cell proliferations to lymphomas with plasmablastic or plasmacytic features.[55] In our 3 patients, monotypic B-cell components with plasmacytoid differentiation were clearly EBV negative. EBV was detected only in small bystander cells in pateint nos 1 and 2, and in association with scattered large cells, likely B-cell blasts, in patient no. 3.

Considering AITL as the most severe diagnosis and the likely determinant of outcome, the clinical evolution of the 3 patients was heterogenous with survivals of 33, 12, and 24 months. The cause of death in patient no. 2 was recurrent AITL a couple of months after complete metabolic remission by CHOP therapy. The evolution of patient nos 1 and 3 was more atypical: both appeared to be cured from the AITL after chemotherapy, but patient no. 1 continued to experience recurrences of the CLL and died in unclear conditions, likely related to long-standing CLL and complications of the BM mini-allograft, while patient no. 3 secondarily developed an AML. This was interpreted as being molecularly unrelated to the AITL, as none of the mutations previously identified in the composite AITL/CLL could be detected in the BM with AML. In particular, *TET2* and *DNMT3A* mutations present in association with AITL and found at lower VAF in a subsequent reactive tissue were suggestive of an underlying CHIP. Nonetheless, no apparent clonal relationship could be demonstrated between the latter and the AML. Another hypothesis could be that of a therapy-induced myeloid neoplasm, despite the absence of any *TP53* gene mutation. Although the time interval between treatment onset with bendamustine and diagnosis of AML was relatively short (19 mo), a similar case has been reported in the literature, with a latency period of only 11 months. The authors suggest that impaired immune surveillance, induced by both CLL and bendamustine, may concur with cytotoxic damage of stem cells to favor the development of AML.[56]

The simultaneous occurrence of distinct lymphomas of both B-cell and T-cell lineages is overall very rare, accounting for only a small proportion of composite lymphomas.[57] Taking into account cutaneous and systemic PTCLs occurring in CLL/SLL patients, <100 cases have been reported in the literature, which is a small number with respect to CLL/SLL prevalence. A large epidemiological study recently confirmed that men with CLL are at increased risk of developing cutaneous T-cell lymphoma in comparison to the general population.[58] T-cell lymphomagenesis has been linked to a perturbation of T-cell homeostasis in CLL. CLL is associated with profound alterations and defects in the immune system and quantitative and qualitative perturbations of T-cell compartments in the blood,[59] and clinical manifestations of decreased immune surveillance and an increased susceptibility to infections. Complex interactions between CLL cells and T cells, leading to chronic T-cell stimulation, result in increased $CD4^+$ and $CD8^+$ T-cell subsets in the blood and accumulation of oligoclonal/monoclonal abnormal T-cell populations.[40] In particular, increased numbers of $CD8^+$ T cells showing increased expression of exhaustion markers (including PD1, CD160, and CD244)[41,60] and of cytotoxic molecules are found in the peripheral blood of patients with CLL.[26] It has been suggested that these abnormal circulating $CD8^+$ clones might be the precursors to the PTCL, NOS with a cytotoxic phenotype, which represent a common histotype of the PTCLs reported in CLL/SLL patients.[19,21,25,26] Frequencies of different types of $CD4^+$ helper T cells have also been found to be increased in CLL patients with the expression of exhaustion markers such as PD1,[60,61] and notably the frequency of TFH cells (which are supportive of CLL cells through the secretion of high levels of IL-21) is increased in the blood and particularly the LN of CLL/SLL patients. Therefore, it could be speculated that these abnormal $CD4^+$ T-cell populations may represent the cell of origin to $CD4^+$ TFH lymphomas, specifically AITL. In addition, exogenous factors such as chemotherapy or radiotherapy used for treating CLL could contribute to the emergence of secondary cancers, a mechanism that may be incriminated in the subset of patients having received earlier therapy for CLL (Table 1).[19,21,23,26,28,32,62] Patient no. 1 had been treated with fludarabine and cyclophosphamide before he developed composite lymphoma. Interestingly, in vitro studies have shown that a combination of these 2 drugs, while reducing the

total number of T cells, induces a more mature phenotype of the residual T cells with enhanced response to mitogenic stimuli.[63] It is therefore possible that therapy could skew the T-cell repertoire and induce a selection of T cells prone to undergo expansion under stimulation.

In cases with simultaneous diagnosis of CLL/SLL and T-cell lymphoma, like in patient nos 2 and 3, it is impossible to determine which of the 2 malignancies developed first, or whether they both developed concurrently, either by chance or due to an underlying genetic predisposition or environmental factor. Given the B-cell supporting properties of TFH cells, it could be hypothesized that AITL could have sustained the expansion of a monoclonal B-cell lymphocytosis into CLL.

Although composite B-cell and T-cell lymphomas represent clonal expansions from distinct lineages, they may be related to a common precursor cell or pluripotent stem cell.[25] An interesting study has shown that inactivation of *DNMT3A* in mouse hematopoietic stem cells induces CLL and PTCL, with distinct methylomes and transcriptomes.[64] A similar scenario can likely be excluded in patient no. 1, where none of the mutations found in the composite tumor (including those in *TET2* which have been found in hematopoietic stem cells in AITL patients)[50] were present either in the initial CLL diagnosis, or in subsequent tissues involved by CLL only. In patient no. 2, a p.R882H *DNMT3A* mutation was found in the LN involved by the composite lymphoma (and in the relapsing AITL), but microdissection failed to produce enough DNA for sequencing of the SLL component alone. In patient no. 3, the truncating *DNMT3A* mutations, detected in the composite infiltrates in LN and BM at the time of diagnosis, were not found in a subsequent BM containing a minimal residual CLL infiltrate. Hence, there is overall no argument in favor of a common precursor in the 3 cases presented here.

In cases of secondary occurrence of PTCL in patients harboring a diagnosis of CLL, the clinical presentation in several instances has been reported to suggest Richter syndrome.[14,16,30,31] In the light of the genetic heterogeneity of "bona fide" Richter syndrome cases, comprising clonally related or unrelated aggressive lymphomas of B-cell lineage, it has been suggested that PTCL cases might be considered under the same umbrella and regarded as a rare variant of Richter syndrome.[13] In our series, patient no. 1 presented with clinical symptoms that indeed suggested Richter syndrome. Whether patient nos 2 and 3 could be assimilated to Richter syndrome is more debatable, because both low-grade and high-grade lymphomatous proliferations were discovered simultaneously; and in patient no. 2 the LN contained SLL (in the absence of peripheral lymphocytosis). However, on biological grounds and for therapeutic purposes, the concept of Richter syndrome is generally extended to include cases with concomitant (in addition to metachronous) diagnosis of aggressive lymphoma, and with SLL (in addition to CLL).[1,9] In conclusion, we report here another type of PTCL that may occur in association with CLL/SLL, adding AITL to the spectrum of rare variants of aggressive neoplasms manifesting as Richter syndrome in CLL/SLL patients.

REFERENCES

1. Swerdlow SH, Campo E, Harris NL, et al. *WHO Classification of Tumours of the Haematopoietic and Lymphoid Tissues*, Revised 4th edition. Lyon, France: IARC; 2017.
2. Jamroziak K, Tadmor T, Robak T, et al. Richter syndrome in chronic lymphocytic leukemia: updates on biology, clinical features and therapy. *Leuk Lymphoma*. 2015;56:1949–1958.
3. Agbay RL, Jain N, Loghavi S, et al. Histologic transformation of chronic lymphocytic leukemia/small lymphocytic lymphoma. *Am J Hematol*. 2016;91:1036–1043.
4. Jain N, Keating MJ. Richter transformation of CLL. *Expert Rev Hematol*. 2016;9:793–801.
5. de Leval L, Vivario M, De Prijck B, et al. Distinct clonal origin in two cases of Hodgkin's lymphoma variant of Richter's syndrome associated With EBV infection. *Am J Surg Pathol*. 2004;28:679–686.
6. Parikh SA, Habermann TM, Chaffee KG, et al. Hodgkin transformation of chronic lymphocytic leukemia: incidence, outcomes, and comparison to de novo Hodgkin lymphoma. *Am J Hematol*. 2015;90:334–338.
7. Xiao W, Chen WW, Sorbara L, et al. Hodgkin lymphoma variant of Richter transformation: morphology, Epstein-Barr virus status, clonality, and survival analysis-with comparison to Hodgkin-like lesion. *Hum Pathol*. 2016;55:108–116.
8. Rossi D, Spina V, Deambrogi C, et al. The genetics of Richter syndrome reveals disease heterogeneity and predicts survival after transformation. *Blood*. 2011;117:3391–3401.
9. Rossi D, Spina V, Gaidano G. Biology and treatment of Richter syndrome. *Blood*. 2018;131:2761–2772.
10. Royle JS, Baade P, Joske D, et al. Risk of second cancer after lymphohematopoietic neoplasm. *Int J Cancer*. 2011;129:910–919.
11. Solomon BM, Chaffee KG, Moreira J, et al. Risk of non-hematologic cancer in individuals with high-count monoclonal B-cell lymphocytosis. *Leukemia*. 2016;30:331–336.
12. Abi-Rafeh J, Beamish IV, Haegert DG, et al. Extranodal NK/T cell lymphoma and lymphomatoid granulomatosis in a patient with chronic lymphocytic leukaemia: case report for a new perspective on Richter syndrome. *Medicine (Baltimore)*. 2020;99:e20106.
13. Roncati L. Richter's syndrome of T-cell lineage (T rex lymphoma). *Curr Med Res Opin*. 2020;36:473–476.
14. Van Der Nest BM, Leslie C, Joske D, et al. Peripheral T-cell lymphoma arising in patients with chronic lymphocytic leukemia. *Am J Clin Pathol*. 2019;152:818–827.
15. Aoyama Y, Kodaka T, Zushi Y, et al. Composite lymphoma as co-occurrence of advanced chronic lymphocytic leukemia/small lymphocytic lymphoma carrying trisomy 12 and t(14;18) and peripheral T-cell lymphoma. *J Clin Exp Hematop*. 2018;58:27–31.
16. Gorodetskiy VR, Probatova NA, Kondratieva TT. Peripheral T-cell lymphoma of the submandibular salivary gland as an unusual manifestation of Richter's syndrome: a case report and literature review. *Case Rep Hematol*. 2017;2017:1262368.
17. Colling R, Royston D, Soilleux E. Transformation of CLL to ALCL: the role of clonality studies in diagnostic molecular haematopathology. *J Hematop*. 2016;9:143–147.
18. Mant S, Taylor G, Dutton D, et al. Development of T-cell lymphomas with an activated cytotoxic immunophenotype, including anaplastic large cell lymphomas, in patients with chronic lymphocytic leukemia: a series of six cases. *Leuk Lymphoma*. 2015;56:774–778.
19. Boyer DF, Lindeman NI, Harris NL, et al. Peripheral T-cell lymphomas with cytotoxic phenotype in patients with chronic lymphocytic leukemia/small lymphocytic lymphoma. *Am J Surg Pathol*. 2014;38:279–288.
20. Persad P, Pang CS. Composite ALK-negative anaplastic large cell lymphoma and small lymphocytic lymphoma involving the right inguinal lymph node. *Pathol Res Pract*. 2014;210:127–129.
21. Alomari A, Hui P, Xu M. Composite peripheral T-cell lymphoma not otherwise specified, and B-cell small lymphocytic lymphoma presenting with hemophagocytic lymphohistiocytosis. *Int J Surg Pathol*. 2013;21:303–308.
22. Suefuji N, Niino D, Arakawa F, et al. Clinicopathological analysis of a composite lymphoma containing both T- and B-cell lymphomas. *Pathol Int*. 2012;62:690–698.

23. Buddula A, Assad D. Peripheral T-Cell lymphoma manifested as gingival enlargement in a patient with chronic lymphocytic leukemia. *J Indian Soc Periodontol*. 2011;15:67–69.
24. Liu T, He M, Carlson DL, et al. ALK-positive anaplastic large cell lymphoma in a patient with chronic lymphocytic leukemia. *Int J Surg Pathol*. 2010;18:424–428.
25. Campidelli C, Sabattini E, Piccioli M, et al. Simultaneous occurrence of peripheral T-cell lymphoma unspecified and B-cell small lymphocytic lymphoma. Report of 2 cases. *Hum Pathol*. 2007;38:787–792.
26. Martinez A, Pittaluga S, Villamor N, et al. Clonal T-cell populations and increased risk for cytotoxic T-cell lymphomas in B-CLL patients: clinicopathologic observations and molecular analysis. *Am J Surg Pathol*. 2004;28:849–858.
27. Martin-Subero JI, Siebert R, Harder L, et al. Cytogenetic and molecular characterization of a patient with simultaneous B-cell chronic lymphocytic leukemia and peripheral T-cell lymphoma. *Am J Hematol*. 2001;68:276–279.
28. Novogrudsky A, Amorosi EL, Gottesman SR. High-grade T-cell lymphoma complicating B-cell chronic lymphocytic leukemia: an unusual manifestation of "Richter's syndrome". *Am J Hematol*. 2001;66:203–206.
29. Lesesve JF, Buisine J, Gregoire MJ, et al. Leukaemic small cell variant anaplastic large cell lymphoma during pregnancy. *Clin Lab Haematol*. 2000;22:297–301.
30. Nai GA, Cabello-Inchausti B, Suster S. Anaplastic large cell lymphoma of the spleen. *Pathol Res Pract*. 1998;194:517–522.
31. Abruzzo LV, Griffith LM, Nandedkar M, et al. Histologically discordant lymphomas with B-cell and T-cell components. *Am J Clin Pathol*. 1997;108:316–323.
32. Lee A, Skelly ME, Kingma DW, et al. B-cell chronic lymphocytic leukemia followed by high grade T-cell lymphoma. An unusual variant of Richter's syndrome. *Am J Clin Pathol*. 1995;103:348–352.
33. Liu YC, Tomashefski JF Jr, Cleveland RP, et al. Composite cutaneous T-cell lymphoma and small B-cell lymphocytic lymphoma: morphologic, immunologic, and molecular genetic documentation of concurrent lymph node involvement. *Mod Pathol*. 1994;7:641–646.
34. Strickler JG, Amsden TW, Kurtin PJ. Small B-cell lymphoid neoplasms with coexisting T-cell lymphomas. *Am J Clin Pathol*. 1992;98:424–429.
35. Singh L, Boulavsky JL, Duvic M. Concurrent chronic lymphocytic leukemia and cutaneous T cell lymphoma: a case series. *Leuk Lymphoma*. 2014;55:2192–2195.
36. Chang MB, Weaver AL, Brewer JD. Cutaneous T-cell lymphoma in patients with chronic lymphocytic leukemia: clinical characteristics, temporal relationships, and survival data in a series of 14 patients at Mayo Clinic. *Int J Dermatol*. 2014;53:966–970.
37. Barzilai A, Trau H, David M, et al. Mycosis fungoides associated with B-cell malignancies. *Br J Dermatol*. 2006;155:379–386.
38. Volk AL, Vannucci SA, Cook W, et al. Composite mycosis fungoides and B-cell chronic lymphocytic leukemia. *Ann Diagn Pathol*. 2002;6:172–182.
39. Hull PR, Saxena A. Mycosis fungoides and chronic lymphocytic leukaemia—composite T-cell and B-cell lymphomas presenting in the skin. *Br J Dermatol*. 2000;143:439–444.
40. Bartik MM, Welker D, Kay NE. Impairments in immune cell function in B cell chronic lymphocytic leukemia. *Semin Oncol*. 1998;25:27–33.
41. Goolsby CL, Kuchnio M, Finn WG, et al. Expansions of clonal and oligoclonal T cells in B-cell chronic lymphocytic leukemia are primarily restricted to the CD3(+)CD8(+) T-cell population. *Cytometry*. 2000;42:188–195.
42. de Leval L, Parrens M, Le Bras F, et al. Angioimmunoblastic T-cell lymphoma is the most common T-cell lymphoma in two distinct French information data sets. *Haematologica*. 2015;100:e361–e364.
43. Dupuy A, Lemonnier F, Fataccioli V, et al. Multiple ways to detect IDH2 mutations in angioimmunoblastic T-cell lymphoma from immunohistochemistry to next-generation sequencing. *J Mol Diagn*. 2018;20:677–685.
44. van Dongen JJ, Langerak AW, Bruggemann M, et al. Design and standardization of PCR primers and protocols for detection of clonal immunoglobulin and T-cell receptor gene recombinations in suspect lymphoproliferations: report of the BIOMED-2 Concerted Action BMH4-CT98-3936. *Leukemia*. 2003;17:2257–2317.
45. Benhattar J, Delacretaz F, Martin P, et al. Improved polymerase chain reaction detection of clonal T-cell lymphoid neoplasms. *Diagn Mol Pathol*. 1995;4:108–112.
46. Dobay MP, Lemonnier F, Missiaglia E, et al. Integrative clinicopathological and molecular analyses of angioimmunoblastic T-cell lymphoma and other nodal lymphomas of follicular helper T-cell origin. *Haematologica*. 2017;102:e148–e151.
47. Lemonnier F, Couronne L, Parrens M, et al. Recurrent TET2 mutations in peripheral T-cell lymphomas correlate with TFH-like features and adverse clinical parameters. *Blood*. 2012;120:1466–1469.
48. Wang C, McKeithan TW, Gong Q, et al. IDH2R172 mutations define a unique subgroup of patients with angioimmunoblastic T-cell lymphoma. *Blood*. 2015;126:1741–1752.
49. Palomero T, Couronne L, Khiabanian H, et al. Recurrent mutations in epigenetic regulators, RHOA and FYN kinase in peripheral T cell lymphomas. *Nat Genet*. 2014;46:166–170.
50. Sakata-Yanagimoto M, Enami T, Yoshida K, et al. Somatic RHOA mutation in angioimmunoblastic T cell lymphoma. *Nat Genet*. 2014;46:171–175.
51. Steinhilber J, Mederake M, Bonzheim I, et al. The pathological features of angioimmunoblastic T-cell lymphomas with IDH2(R172) mutations. *Mod Pathol*. 2019;32:1123–1134.
52. Gaulard P, de Leval L. Follicular helper T cells: implications in neoplastic hematopathology. *Semin Diagn Pathol*. 2011;28:202–213.
53. de Leval L, Gisselbrecht C, Gaulard P. Advances in the understanding and management of angioimmunoblastic T-cell lymphoma. *Br J Haematol*. 2010;148:673–689.
54. Nagoshi H, Kuroda J, Kobayashi T, et al. Clinical manifestation of angioimmunoblastic T-cell lymphoma with exuberant plasmacytosis. *Int J Hematol*. 2013;98:366–374.
55. Balague O, Martinez A, Colomo L, et al. Epstein-Barr virus negative clonal plasma cell proliferations and lymphomas in peripheral T-cell lymphomas: a phenomenon with distinctive clinicopathologic features. *Am J Surg Pathol*. 2007;31:1310–1322.
56. Garcia-Munoz R, Garcia DK, Roldan-Galiacho V, et al. Therapy-related acute myeloid leukemia in a patient with chronic lymphocytic leukemia treated with rituximab-bendamustine. *Ann Hematol*. 2014;93:699–702.
57. Kuppers R, Duhrsen U, Hansmann ML. Pathogenesis, diagnosis, and treatment of composite lymphomas. *Lancet Oncol*. 2014;15:e435–e446.
58. Chang TW, Weaver AL, Shanafelt TD, et al. Risk of cutaneous T-cell lymphoma in patients with chronic lymphocytic leukemia and other subtypes of non-Hodgkin lymphoma. *Int J Dermatol*. 2017;56:1125–1129.
59. Roessner PM, Seiffert M. T-cells in chronic lymphocytic leukemia: guardians or drivers of disease? *Leukemia*. 2020;34:2012–2024.
60. Riches JC, Davies JK, McClanahan F, et al. T cells from CLL patients exhibit features of T-cell exhaustion but retain capacity for cytokine production. *Blood*. 2013;121:1612–1621.
61. Novak M, Prochazka V, Turcsanyi P, et al. Numbers of CD8+PD-1+ and CD4+PD-1+ cells in peripheral blood of patients with chronic lymphocytic leukemia are independent of binet stage and are significantly higher compared to healthy volunteers. *Acta Haematol*. 2015;134:208–214.
62. Sluzevich JC, Hall MR, Roy V. Subcutaneous panniculitis-like T-cell lymphoma after rituximab. *J Am Acad Dermatol*. 2012;67:e223–e225.
63. Gassner FJ, Weiss L, Geisberger R, et al. Fludarabine modulates composition and function of the T cell pool in patients with chronic lymphocytic leukaemia. *Cancer Immunol Immunother*. 2011;60:75–85.
64. Haney SL, Upchurch GM, Opavska J, et al. Loss of Dnmt3a induces CLL and PTCL with distinct methylomes and transcriptomes in mice. *Sci Rep*. 2016;6:34222.